SEISMIC ASSESSMENT AND COST-EFFECTIVENESS OF HIGH-RISE BUILDINGS WITH INCREASING CONCRETE STRENGTHS

A.M. Mwafy, N. Hussain & K. El-Sawy
United Arab Emirates University, PO Box 17555, Al Ain, UAE

ABSTRACT:
The impact of increasing material strength on seismic performance and cost-effectiveness of high-rise buildings is investigated in this paper. Five 60-story reinforced concrete buildings with varying concrete strengths, ranging from 45 to 110 MPa, are designed and detailed to fine accuracy keeping almost equal periods of vibration. Detailed fiber-based simulation models are developed to assess the seismic response of the reference structures using inelastic pushover and incremental dynamic analyses (IDAs) under the effect of 20 input ground motions. It is concluded that a considerable saving in construction cost and gain in useable area are attained with increasing concrete strength. The seismic response of high-strength tall structures is not inferior, but may be safer at high ground motion intensity levels, than that of normal strength materials. The paper summarizes a systematic seismic assessment study and provides practical recommendations to understand the reliability and cost effectiveness of high-rise buildings in earthquake-prone regions.

Keywords: High-strength concrete, high-rise buildings, cost effectiveness, seismic response, IDA.

1. INTRODUCTION

The use of high-strength materials is promoted in high-rise buildings to effectively use floor areas, control vibrations and expedite construction. The rapid increase in the cost of land in urban centers and availability of high-strength materials resulted in a significant increase in high-rise building construction. For instance, the United Arab Emirates has witnessed a large demand in high-rise buildings in recent years which led the designers to effectively utilize high-strength concrete and steel. Although the engineering understanding of the performance of high-strength reinforced concrete (RC) structures under static loading is well-developed, little information is available on the economics of high-rise buildings and their performance under earthquake loading. This emphasizes the need to investigate the behavior of high-rise structures when designed to different material strengths under the effect of earthquake loads which control the design of a wide range of tall buildings.

The seismic performance of high-rise buildings is assessed in the present study through fragility relationships. Different approaches can be used to derive fragility functions (e.g. Rossetto and Elnashai 2005). The approach of generating damage data through analytical simulations is the most realistic option, particularly for the UAE, and hence it is adopted in the present study (Mwafy 2012). Several techniques for deriving vulnerability curves based on the numerically simulated structural damage statistics have been also proposed in the literature, with a diversity in structural idealizations, analysis methods, seismic hazard and damage models. Most of these techniques require a large number of analyses to account for uncertainty. This is particularly true when adopting multi-degree-of-freedom inelastic dynamic simulations for deriving the vulnerability relationships, which is the approach adopted herein. The present study aims at investigating the relationship between seismic performance and cost-effectiveness of tall buildings through designing and developing detailed simulation models for high-rise buildings with various concrete grades, ranging from 45 to 110 MPa. The construction cost is compared in terms of steel, concrete and formwork. Over 1600 inelastic

pushover analyses (IPAs) and incremental dynamic analyses (IDAs) are performed using 20 natural and artificial earthquake records to derive vulnerability relationships and to provide insights into the seismic response of the reference structures up to collapse.

2. DESIGN AND MODELING OF REFERENCE STRUCTURES

Five 60-story RC buildings (denoted as M1, M2, M3, M4 and M5) are selected and fully designed for the purpose of the current study. The referred five buildings have the same layout shown in the Figure 1(b), which represents the architectural layouts commonly adopted for high-rise buildings in the UAE. Each building comprises of two basements (B1 and B2), a ground story (L1) and 57 typical stories (L2 to L58). The typical height of all floors is 3.2 meters except for the ground story, which is 4.5 meters. The total height for each of the five buildings is therefore 193.3 meters. The permanent loads used in design include the self-weight of structural members in addition to a uniformly distributed load on slab of 4.0 kN/m^2, which accounts for other dead loads (partitions, flooring, etc.). The live load is 2.0 kN/m^2 except for stairs and exit ways, which is 4.8 kN/m^2. Wind loads are estimated from ASCE 7-10 (ASCE 2010) with a basic wind speed of 45 m/s and an exposure category C. The most recent mapped spectral acceleration parameters for the UAE are used to calculate seismic loads according to ASCE 7-10 (ASCE 2010). The five buildings are proportioned and detailed according to various load combinations and the design provisions recommended by the ACI 318 building code (ACI 2005) such that they have the same periods of vibration. The floor slab systems comprise of 0.28 m cast in situ flat slabs for all floors with its thickness and reinforcement selected to prevent undesirable modes of failure. Yield strength of steel reinforcement is 460 MPa. Constant concrete cube strength of 45 MPa is used for floor slabs, while the concrete strength varies along the height of shear walls and core walls from 45 MPa to 110 MPa (cylinder strength, f_c', of 35 MPa to 95 MPa, respectively). The cross-sections of shear walls and the thickness of core walls are reduced every five stories along the building height. Table 1 and Figures 2&3 present sample results from this extensive design process.

Table 1. Elastic periods, material strengths and sizes of main structural members of reference buildings

Ref.	Period, sec	Member Name		Characteristics	Story					
					B1-L8	L9-L18	L19-L28	L29-L38	L39-L48	L49-L58
M1	6.879	Walls	P2, P5, P6	Cross section	650 x 4750	600 x 4750	500 x 4750	400 x 4750	300 x 4750	275 x 4750
				f_c'	50	40	35	35	35	35
		Core	C1	Thickness	550	450	350	300	275	275
				f_c'	40	35	35	35	35	35
			C2	Thickness	600	500	400	350	300	275
				f_c'	40	35	35	35	35	35
M2	6.829	Walls	P2, P5, P6	Cross section	600 x 4750	550 x 4750	450 x 4750	350 x 4750	275 x 4750	250 x 4750
				f_c'	57	50	40	40	35	35
		Core	C1	Thickness	500	400	300	275	250	250
				f_c'	50	40	40	35	35	35
			C2	Thickness	550	450	350	300	275	250
				f_c'	50	40	40	35	35	35
M3	6.810	Walls	P2, P5, P6	Cross section	550 x 4750	500 x 4750	400 x 4750	325 x 4750	250 x 4750	225 x 4750
				f_c'	65	57	50	50	40	35
		Core	C1	Thickness	450	350	275	250	225	225
				f_c'	57	50	50	40	40	35
			C2	Thickness	500	400	300	275	250	225
				f_c'	57	50	50	40	40	35
M4	6.831	Walls	P2, P5, P6	Cross section	500 x 4750	450 x 4750	350 x 4750	300 x 4750	225 x 4750	200 x 4750
				f_c'	75	65	57	57	50	40
		Core	C1	Thickness	400	300	250	225	200	200
				f_c'	65	57	57	50	50	40
			C2	Thickness	450	350	275	250	225	200
				f_c'	65	57	57	50	50	40
M5	6.886	Walls	P2, P5, P6	Cross section	450 x 4750	400 x 4750	300 x 4750	250 x 4750	225 x 4750	200 x 4750
				f_c'	95	85	75	75	57	40
		Core	C1	Thickness	300	275	250	225	200	200
				f_c'	85	75	75	57	57	40
			C2	Thickness	400	300	275	250	225	200
				f_c'	85	75	75	57	57	40

Steel yield strength = 460 MPa;Vertical steel reinforcement ratio of walls and cores vary from 1.0% to 4.6% along the height of the buildings
Flat slab thickness = 0.28mm; concrete strength is in MPa and dimensions are in mm.

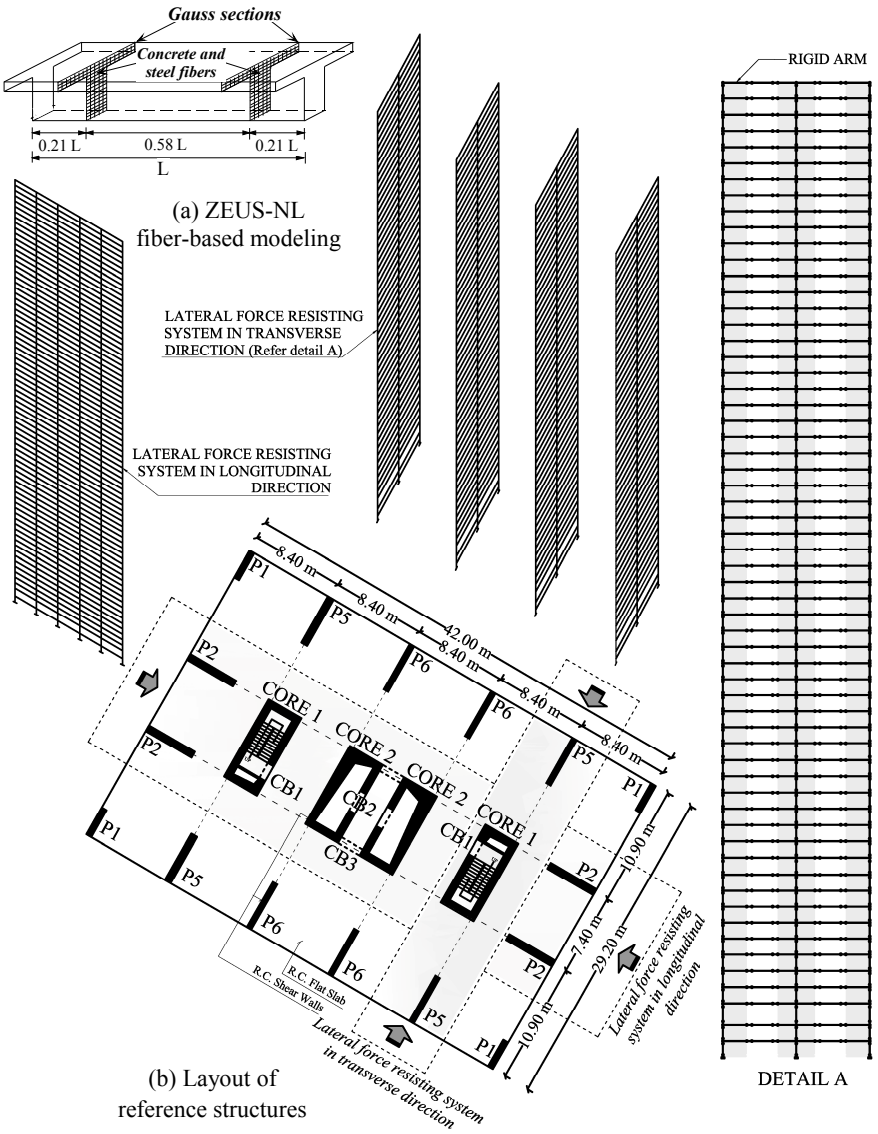

Figure 1. Modeling approach of reference structures for inelastic analysis: (a) ZEUS-NL fiber-based models in the longitudinal and transverse directions, and (b) building layout

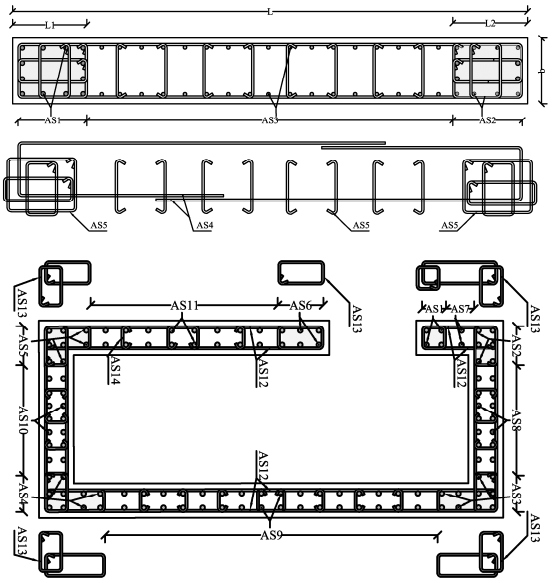

Figure 2. Sample reinforcement details

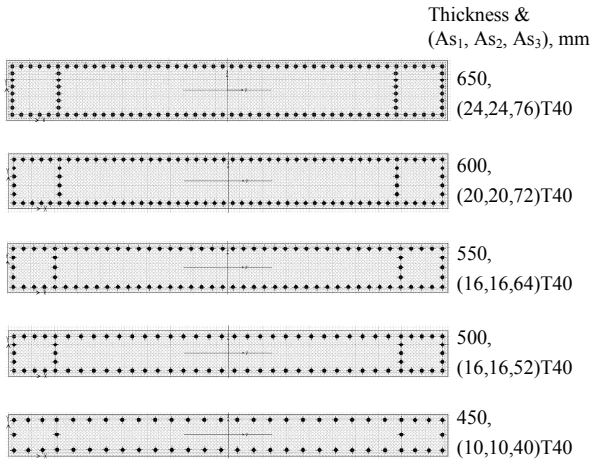

Figure 3. Steel reinforcement and cross section of P5 and P6 (M1 to M5 from top to bottom, respectively)

The idealization adopted in the current study effectively models reinforcing steel, unconfined and confined concrete and is performed using ZEUS-NL (Elnashai et al. 2012). This approach allows monitoring the stress-strain response at each fiber over two Gauss sections through the integration of the nonlinear stress-strain response of different fibers in which the section is subdivided, as shown in Figure 1(a). This modeling approach reduces the modeling uncertainty since the assumptions required by other analysis platforms such as the moment-curvature relationships are avoided. A number of cubic elasto-plastic elements capable of representing the spread of yielding and cracking are used to model each structural member. This enables modeling different arrangements of reinforcing steel along the length of each structural member as specified in design. Rigid arms are also utilized to connect the slab/beam ends with shear walls, as shown in Figure 1 (a). Actual material strengths are employed in the ZEUS-NL models. The concrete response is represented by using a uniaxial constant confinement concrete model, while a bilinear elasto-plastic model is selected to model reinforcing steel. Three-dimensional modeling and analysis of high-rise structures are computationally demanding, particularly with the wide range of reference buildings and input ground motions considered in the present study. A two-dimensional idealization is therefore adopted to develop fragility relationships using IDCAs. It is assumed that for each building four framing systems resist seismic forces in the transverse directions, while one frame resist lateral forces in the longitudinal direction, as shown in Figure 1. Each of the framing systems in the transverse direction is loaded with 25% of the total mass of the building. It is noteworthy that the selection of the reference structures layout was motivated by the desire to arrive at comparable lateral capacity in the two orthogonal horizontal directions. Results obtained from the 3D ETABS (CSI 2011) models developed for the design of the reference buildings and from previous vulnerability assessment studies carried out on a comparable building layout indicated that the transverse direction is slightly more vulnerable than the longitudinal direction (e.g. Mwafy 2011). Therefore, the present study only focuses on the framing systems in the transverse direction to reduce the number of IDAs.

3. COMPARATIVE COST ASSESSMENT

The cost of the five reference structures is calculated with respect to the costs of concrete, reinforcement and formwork. Other architectural and finishing costs are considered to be constant between all reference structures. Material quantities of structural elements are estimated based on the detailed design, as discussed above, and their respective costs are evaluated. The area gained due to the reduction in the dimensions of vertical elements with increasing concrete strength is computed and the net profit is evaluated considering the overall cost and the cost of land. Figure 4 summarizes the total cost saving of concrete, steel and formwork, while Figure 5 shows a comparison of sealable area profit due to the additional area obtained from the reduction in cross sections. The total profits gained from increasing the saleable area along with the saving in construction cost due to increasing material strength are depicted in Figure 6. All results are presented relative to building M1, which has the lowest concrete strength. It is noteworthy that the material costs depend to a large extent on the cost of reinforcing steel, as shown from Figure 4. It is noted that the cost of steel reinforcement significantly reduces by 37% with the use of high-strength concrete in Building M5 compared with those calculated for M1. The results indicate that increasing the concrete strength generally results in the most cost effective design due to the reduction in section sizes and increasing saleable area. For building M5, the total profit gained from using high strength material is $4.77 million higher than that of M1. Comparisons of the increase in profit with the seismic performance of the reference structures is presented in subsequent sections.

4. UNCERTAINTY MODELING

The UAE seismicity is characterized by earthquakes originated from different seismic sources, namely long-distance events from Southern Iran along with earthquakes from local seismic faults. Due to the lack of real strong records for the UAE, 20 earthquake records were selected from ground motion databases to represent far-field seismic events (Ambraseys et al. 2004; PEER 2012). The records

represent severe distant earthquakes of magnitude ranging from 6.93 to 7·62 with 95 km to 160 km epicentral distance. The input ground motions were selected based on the distance to source, magnitude and spectral amplification to fit the uniform hazard spectrum (UHS) for Dubai for 10% probability of exceedance in 50 years, as shown in Figure 7. This seismic scenario along with another near-field seismic scenario were recommended in a previous seismic hazard assessment study for Dubai (Mwafy et al. 2006). Moreover, recent vulnerability assessment studies carried out on multi-story buildings concluded that the far-field seismic scenario has much higher impact on the response of buildings with different heights (Mwafy 2011; Mwafy 2012). The present study thus focuses on the severe distant earthquake scenario, as shown in Figure 7. The selected input ground motions are scaled to a design peak ground acceleration (PGA) of 0.16g, which was recommended for Dubai (Mwafy et al. 2006), and its multiples. The selected records account for the uncertainty of ground motion which is the most significant source of uncertainty (e.g. Porter et al. 2002). It is also important to note that the detailed fiber-based modeling approach and analysis procedure (IDA) adopted for deriving the vulnerability curves significantly contribute in reducing uncertainties compared with other alternatives.

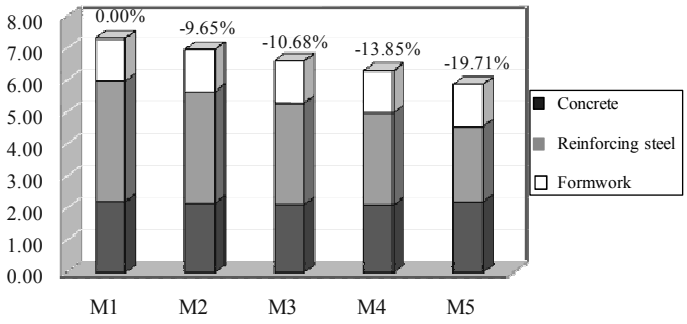

Figure 4. Cost saving of materials and formwork relative to building M1

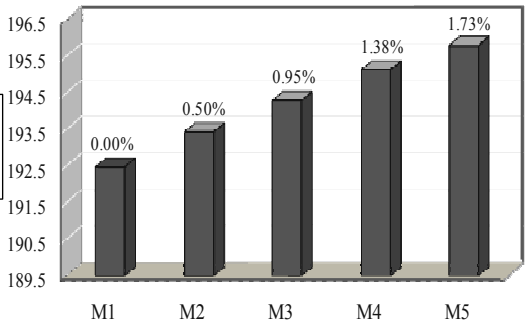

Figure 5. Comparison of total sealable area profit relative to building M1

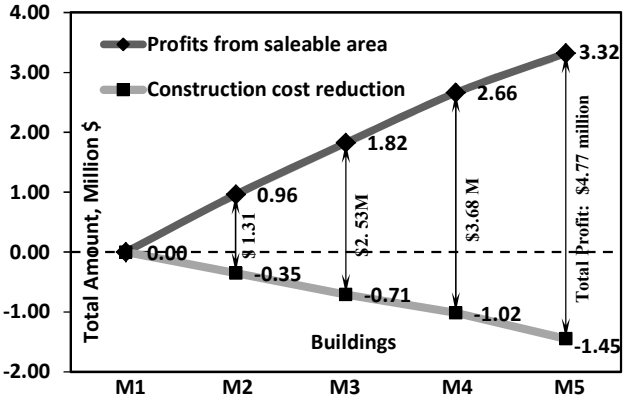

Figure 6. Profits gained from increasing saleable area and saving of material cost relative to building M1

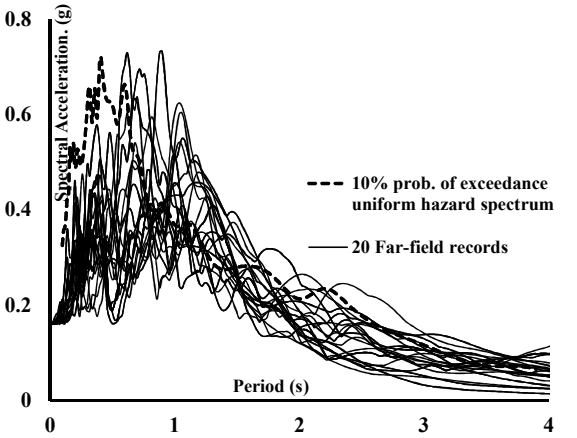

Figure 7. Response spectra of 20 input ground motions representing far-field seismic scenario along with UHS for Dubai

5. PERFORMANCE INDICATORS AND SCALING APPROACH

Three performance limit states are adopted in the present study for the derivation of vulnerability curves, namely: (i) Immediate Occupancy 'IO', (ii) Life Safety 'LS', and Collapse Prevention 'CP' (ASCE 2006). The interstory drift ratio (IDR) is considered as the primary performance criterion to evaluate the damage states of the reference structures. For concrete wall structures, the three performance levels adopted by ASCE/SEI 41-06 (ASCE 2006) are 0.5%, 1.0% and 2.0%, which are

related to minor cracking (IO), extensive damage (LS), and extensive concrete crushing and buckling of reinforcement (CP), respectively. The code recommended drift limits tend to be on the conservative side. Less conservative IDRs have been recommended in the literature based on analytical and experimental results. For instance, for ductile concrete wall structures, Ghobarah (2004) proposed IDR limits associated with 'no damage', 'light reparable damage', 'irreparable damage or yield point', 'severe damage or life safe', and 'collapse' to be <0.2%, 0.4%, >0.8%, 1.5%, and >2.5%, respectively. Following these recommendations, a CP performance level of 2.5% is therefore adopted in the present study.

To estimate the above stated IO and LS performance limit states, IPAs are conducted for the five reference structures to trace the sequence of yielding and the progress of the capacity curve up to the collapse limit state. Following the recommendations of modern design guidelines, two lateral load distributions are employed in IPA, namely the uniform and the inverted triangular load patterns (ASCE 2006). Previous studies on high-rise buildings concluded that the uniform lateral load can be conservatively used for estimating the initial stiffness and lateral capacity (e.g. Mwafy et al. 2006; Mwafy 2011). For a building to be occupied immediately after the earthquake with little or no repair, it should remain in the elastic range so that non-structural components are not significantly damaged. First yield is typically assumed when the strain in the main longitudinal tensile reinforcement exceeds the steel yield strain. The IDRs at the first indication of yield is considered as the IO limit states. The adopt IO performance limit are 0.77%, 0.78%, 0.78%, 0.78% and 0.79% for the M1 to M5 buildings, respectively. These are the most conservative values obtained from both IPAs and IDAs. The LS limit state, which falls between the IO and CP, represents a 'significant damage' sustained by the structure, while it accounts for a reasonable margin of safety against collapse. This margin is considered in ASCE/SEI 41-06 (2006) as 50% of the CP limit state. In the present study, the starting point of the post-elastic branch (global yield threshold) is considered as the LS limit states. This value is 1.35%, 1.32%, 1.30%, 1.28% and 1.27% for the M1 to M5 buildings, respectively. The adopted IO, LS and CP limit states are generally consistent with previous studies. On the basis of the adopted limit states, extensive IDAs are performed with 20 natural and artificial ground motions to derive the fragility curves as described in the following sections.

The choice of a measure for ground motion intensity is important for the accurate representation of the statistics along the horizontal axis of the fragility curve. Several intensity measures were recommended in previous studies such as Peak Ground Acceleration (PGA) and Spectral Acceleration (SA). The selected ground motions represent certain seismic scenario. Scaling these ground motions using their PGAs relates the seismic forces directly to the input accelerations. This simple scaling method agrees with the approach adopted by design codes, and hence it was employed in several previous studies and in the present work (e.g. Kwon and Elnashai 2006). The selected input ground motions are scaled using their PGA to derive vulnerability relationships based on the expression proposed by Wen et al. (2004). The IDAs are carried out for all reference structures up to the satisfaction of different limit states. Each of the 20 input ground motions is scaled up using an incrementing scaling factor of 0.08g, which represents half the design PGA according to the study of Mwafy et al. (2006). Fifteen time history analyses are conducted for each building-input ground motion, starting from a PGA of 0.08g and ending with a PGA of 1.20g, to attain all limit states and improve the resolution of the vulnerability curves, as shown in Figure 8.

6. DERIVATION OF FRAGILITY RELATIONSHIPS USING IDA

Vulnerability relationships of the five reference structures are derived using IDAs under the effect of the 20 natural and artificial ground motions. Local and global response parameters are monitored throughout the scaling range (0.08g to 1.20g), as discussed above. A total of 300 points are plotted for each reference building, each point represents a PGA-IDR value obtained from an inelastic response history analysis. Regression analyses are carried out to derive the power law equation required for deriving the fragility relationships. Figure 8 depicts a sample of IDA results for building M5. The statistical distributions obtained from the over 1500 IDAs carried out for the five reference structures

are used to calculate the probability of exceeding each limit state at different intensity levels. The vulnerability curves are derived by plotting the calculated probability data versus PGAs. Figure 8 shows the derived fragility relationships of building M5, while Figure 9 compares between the fragility curves of the reference structures at different limit states using the methodology outlined above.

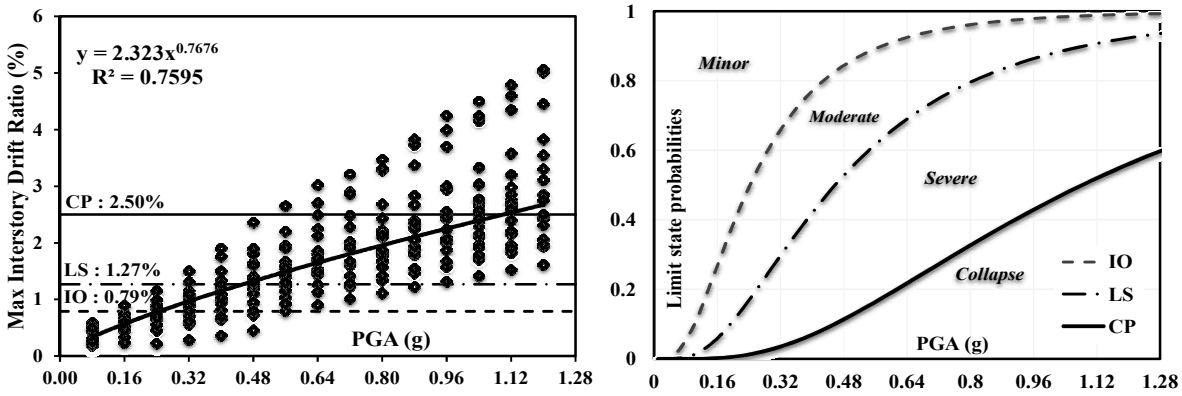

Figure 8. Selected IDA results and fragility relationships for building M5

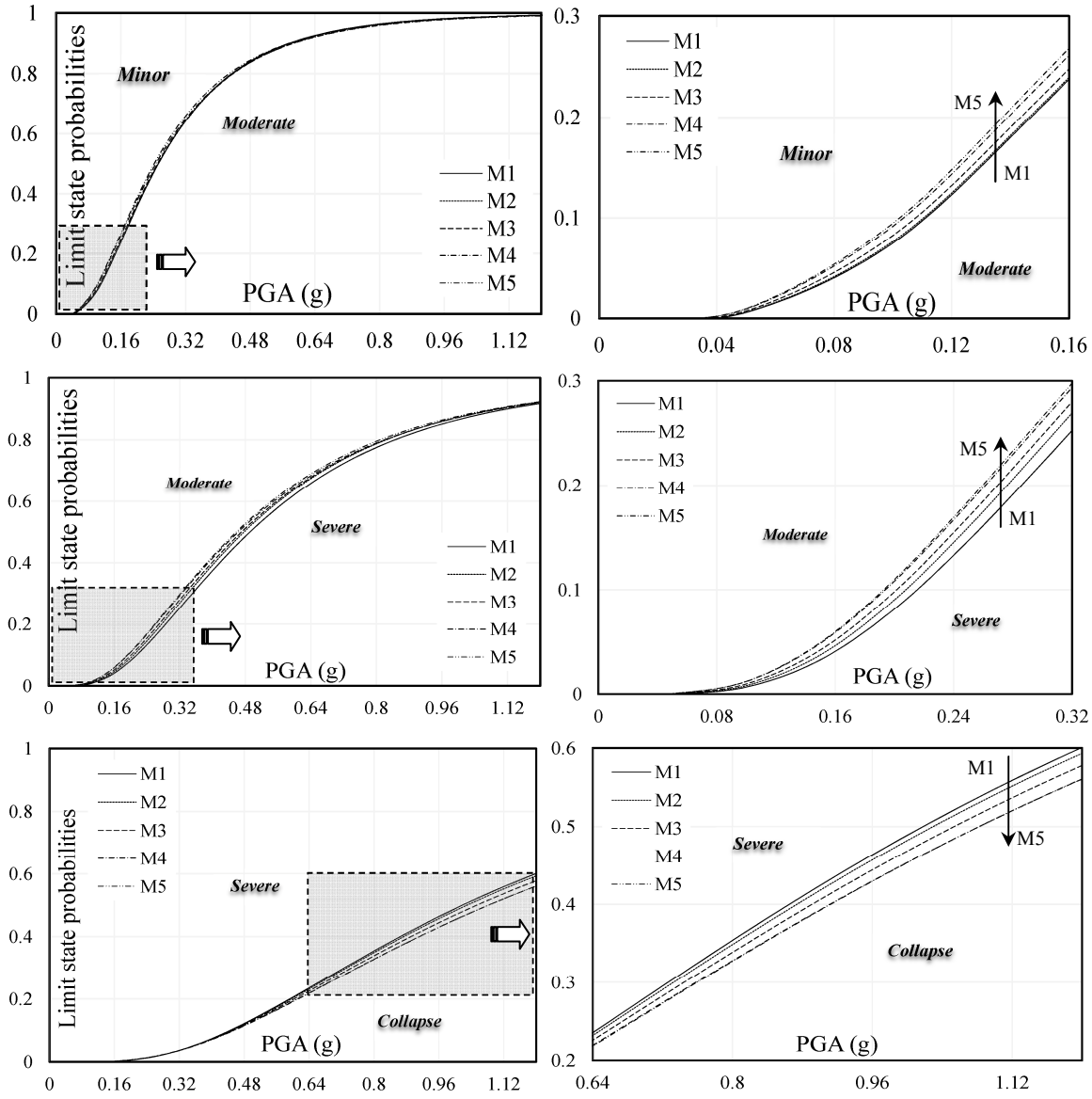

Figure 9. Fragility curves of the reference structures at the IO (top), LS (middle) and CP (bottom) limit states

It is clear from Figure 8 that the steepness of the developed fragility curves increases from CP to IO. For the IO and LS limit states, it is shown from Figure 9 that the slops are slightly steeper and the probability of exceeding limit states is higher for higher strength concrete buildings (e.g. building M5) compared with their lower material strength counterparts (e.g. building M1). This unlike the case of the CP limit state in which the probability of exceeding this limit state decreases with increasing material strength. The enhancement in the seismic response of the higher material strength buildings at the CP limit state is attributed to controlling drift at high ground motion intensities. Limit state probabilities of the reference buildings at four PGA levels, namely 0.16g, 0.32g, 0.64g and 1.12g, are calculated from fragility curves. The damage state probabilities shown in Figure 10 are determined at the above-mentioned PGA levels by calculating the differences between limit state probabilities. It is shown that at the design PGA (i.e. 0.16g), the probability of moderate damage in generally less than 20%, while the probability of severe damage is very low. It is important to note that ordinary buildings are designed to experience certain level of damage at the design intensity. The high probability of no/minor damage is a clear indication for the satisfactory performance of the reference structures under the most conservative seismic scenario for Dubai. At twice the design PGA (i.e. 0.32g), the probability of moderate and severe damage are less than 40% and 27%, respectively, while the probability of collapse is negligibly small. The results indicate that the performance of the five reference structures is acceptable at twice the design PGA.

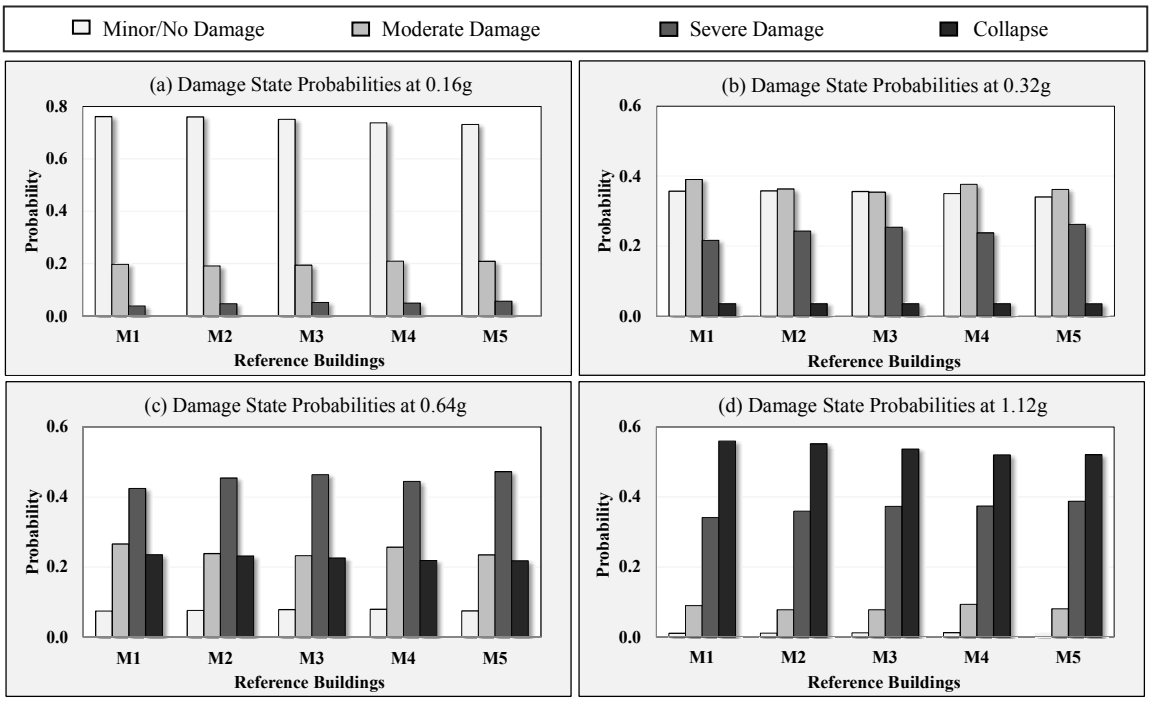

Figure 10. Damage state probabilities at different input ground motion levels

Figure 10 shows that the response of the five reference structures is comparable. Certain damage states slightly increases with increasing material strength, while other damage states slightly decreases. It is also clear from Figure 10(d) that the probability of collapse slightly decreases with increasing material strength. The number of plastic hinges formed in horizontal and vertical structural members at twice the design PGA is shown in Figure 11. It is shown that the number of hinges in horizontal members slightly increases with increasing concrete strength, while marginal desirable changes are observed in vertical members. This indicates that the spread of inelasticity in shear walls is almost unaffected by the change in concrete strength. The local response of the reference structures shown in Figure 11 confirms that the slight increase in certain damage states due to increasing material strength, particularly at lower PGA levels as indicated in Figure 9 and 10, does not cause any undesirable consequences in vertical members. The results presented in Figures 9 to 11 confirms that the behavior of high strength concrete structures is not inferior, and may exceed at certain PGA levels, that of normal strength materials.

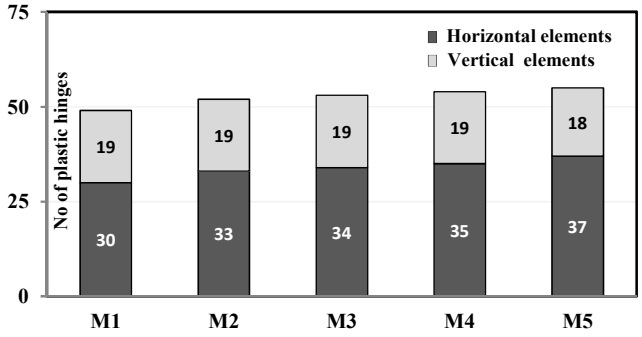

Figure 11. Plastic hinge formation in horizontal and vertical structural elements of the reference buildings at 0.32g (average results of all input ground motions)

7. OVERALL IMPACT ON PROFIT AND PERFORMANCE

The profit from saleable area after deducting all expenses incurred in the construction, including the cost of land, is estimated for the reference buildings relative to building M1. As indicated in Figure 6, the profit consistently increases with increasing concrete strengths. This profit is compared with different global damage states calculated from the fragility relationships relative to building M1. Sample of the relationships between profits and performance at different PGA levels is presented in Figure 12. It is shown from Figure 12(a) that at a PGA of 0.32g, the probability of moderate damage decreases for all buildings when compared with M1. It is also clear that the probability of reaching collapse at a PGA of 1.12g consistently decreases from building M1 to M5, as shown from Figure 12(b). The overall increase in profit and improvement in performance (i.e. reduction in damage) relative to M1 is significant, as shown in Figure 12. The overall improvement in profit-performance exceeds 10% for building M5. The presented results confirm that the seismic response of high-strength concrete tall buildings is comparable to that of normal strength materials for all damage states and at all PGA levels. Increasing concrete strengths provides a considerable profit, which is accompanied in several cases with enhancements in seismic performance.

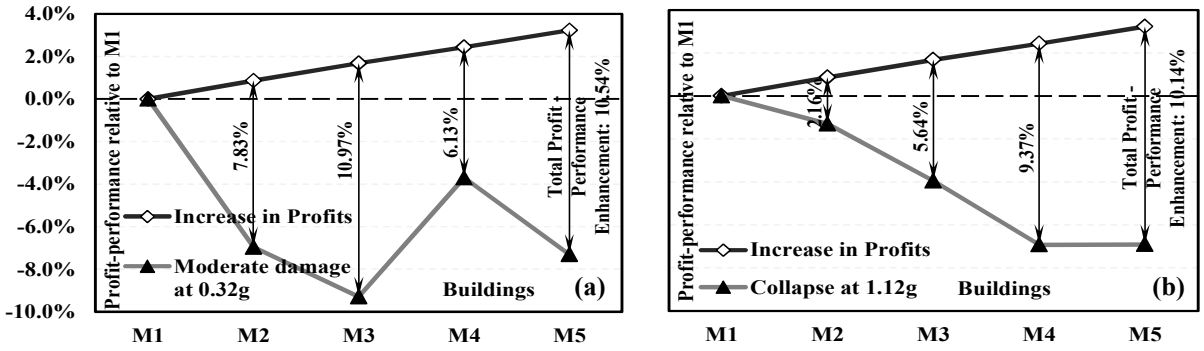

Figure 12. Overall impact on profit-performance with increasing material strength: (a) moderate damage state vs profits at twice the design PGA, and (b) collapse vs profits at 1.12 g

8. CONCLUSIONS

This paper investigated the impact of increasing material strength on seismic performance and cost-effectiveness of high-rise buildings. The study included the structural design and numerical modeling of five 60-story structures representing contemporary high-rise buildings with varying concrete strengths, ranging from 45 to 110 MPa. The comprehensive structural design and detailing of the reference structures to the most recent building codes insured that almost equal periods of vibration were obtained for all buildings. This enabled the effective assessment and comparison of seismic

performance and cost from different designs. Over 1600 inelastic pushover analyses (IPAs) and incremental dynamic analyses (IDAs) were carried out using detailed fiber-based simulation models and 20 earthquake records. Limit states were selected based on local and global response and used to derive the vulnerability relationships of the reference structures. The statistical distributions obtained from IDA results were used to calculate the probability of exceeding different limit states at different ground motion intensity levels. Increasing the concrete strength generally results in the most cost effective design due to the reduction in section sizes and increasing saleable area. The total profit gained from using the highest material strength was $4.77 million when compared with the building that has the lowest concrete strength. The net profit, which was calculated from saleable area after deducting all construction expenses and cost of land, consistently increased with increasing concrete strengths. The seismic performance of the five reference structures was comparable and acceptable at both the design and twice the design PGA. Some damage states slightly increased with increasing material strength, particularly at lower PGA levels, while other damage states slightly decreased. Monitoring the local response confirmed that the minor increase of certain damage states did not cause any undesirable consequences in vertical members. It was concluded that the behavior of high strength concrete structures is not inferior, and may exceed at high ground motion intensity levels, that of normal strength materials. The overall improvement in profit-performance from increasing concrete strength exceeded 10%, which is significant considering the total value of high-rise buildings.

AKCNOWLEDGEMENT

This work was partially supported by the United Arab Emirates University under research grant RSA-1108-00163.

REFERENCES

ACI (2005). Building Code Requirements for Structural Concrete and Commentary (318-05). *American Concrete Institute, Detroit, Michigan.*

Ambraseys, N.N., Douglas, J., Sigbjornsson, R., Berge-Thierry, C., Suhadolc, P., Costa, G. and Smit, P.M. (2004). *Dissemination of European strong-motion data, vol. 2, using strong-motion datascape navigator, CD ROM collection*, Engineering and Physical Sciences Research Council, Swindon, UK, Feb. 2004

ASCE (2006). *Seismic rehabilitation of existing buildings, ASCE Standard ASCE/SEI 41-06 "formerly FEMA 356"*, American Society of Civil Engineers, Reston VA

ASCE (2010). *Minimum design loads for buildings and other structures, ASCE Standard ASCE/SEI 7-10*, American Society of Civil Engineers, Reston, VA

CSI (2011). *ETABS - Integrated building design software*, Computers and Structures, Inc., Berkeley, California

Elnashai, A.S., Papanikolaou, V. and Lee, D. (2012). *Zeus-NL - A System for Inelastic Analysis of Structures - User Manual,* , Mid-America Earthquake Center, Univ. of Illinois at Urbana-Champaign, Urbana, IL

Ghobarah, A. (2004). *On drift limits associated with different damage levels*, Proceedings of the International Workshop on Performance-Based Seismic Design Concepts and Implementation, Bled, Slovenia, Pacific Earthquake Engineering Research Center Report 2004/05.

Kwon, O.S. and Elnashai, A.S. (2006). The effect of material and ground motion uncertainty on the seismic vulnerability curves of RC structure. *Engineering Structures* **28: 2**, 289-303.

Mwafy, A., Elnashai, A., Sigbjörnsson, R. and Salama, A. (2006). Significance of severe distant and moderate close earthquakes on design and behavior of tall buildings. *The Structural Design of Tall and Special Buildings* **15: 4**, 391-416.

Mwafy, A.M. (2011). Assessment of seismic design response factors of concrete wall buildings. *Earthquake Engineering and Engineering Vibration* **10: 1**.

Mwafy, A.M. (2012). Analytically-derived fragility relationships for the modern high-rise buildings in the UAE. *Structural Design of Tall and Special Buildings*, In Press (published online).

PEER (2012). *PEER NGA database*, Pacific Earthquake Engineering Research Center, University of California, Berkeley, California

Porter, K., Beck, J. and Shaikutdinov, R. (2002). Sensitivity of building loss estimates to major uncertain variables. *Earthquake Spectra* **18(4): 719-743**.

Rossetto, T. and Elnashai, A.S. (2005). A new analytical procedure for the derivation of displacement-based vulnerability curves for populations of RC structures. *Engineering Structures* **27: 3**, 397-409.

Wen, Y.K., Ellingwood, B.R. and Bracci, J. (2004). *Vulnerability function framework for consequence-based engineering*, University of Illinois at Urbana-Champaign, Urbana.